THE LATERAL DISTRIBUTION OF PYRENE-LABELED SPHINGOMYELIN AND GLUCOSYLCERAMIDE IN PHOSPHATIDYLCHOLINE BILAYERS

R. C. HRESKO,* I. P. SUGÁR,*‡ Y. BARENHOLZ,*§ AND T. E. THOMPSON*
*Department of Biochemistry, University of Virginia School of Medicine, Charlottesville, Virginia 22908; ‡Institute of Biophysics, Semmelweis Medical University, Budapest 1444, Hungary; and §Department of Biochemistry, The Hebrew University, Hadassah Medical School, Jerusalem, Israel

ABSTRACT The lateral distribution of *N*-[10(1-pyrenyl)decanoyl]-sphingomyelin (PyrSPM) and *N*-[10(1-pyrenyl)decanoyl]-glucocerebroside (PyrGlcCer) was studied in multilamellar vesicles of 1,2-dipalmitoyl-, 1,2-dimyristoyl-, and 1-palmitoyl-2-oleoyl-phosphatidylcholine (DPPC, DMPC, and POPC, respectively) under anaerobic conditions by determining the excimer-to-monomer fluorescence intensity ratio (E/M) as a function of temperature. The $E/M(T)$ curves for PyrSPM and PyrGlcCer in the three phosphatidylcholine matrices are qualitatively similar to the curves reported for 1-palmitoyl-2-[10-(1-pyrenyl)decanoyl]-phosphatidylcholine (PyrPC) in the same three matrix phospholipids (Hresko, R. C., I. P. Sugár, Y. Barenholz, and T. E. Thompson, 1986, *Biochemistry*, 25:3813–3823). However, there is independent evidence to suggest that sphingomyelin and glucocerebroside are organized in POPC, DPPC, and DMPC in a more complex manner than is PyrPC. In an effort to examine further the relationship between the lateral distribution of the labeled lipid and the shape of an $E/M(T)$ curve, E/M vs. temperature simulations were carried out together with an analysis of the equation that relates E/M to the system parameters. The results indicate that information about the lateral distribution of the pyrene-labeled lipid can be obtained from an $E/M(T)$ curve only for those systems in which the gel to liquid crystalline phase transition temperature of the matrix lipid is higher than that of the pyrene-labeled lipid. However, very little can be known about the system from an $E/M(T)$ curve if the matrix lipid has the lower phase transition temperature.

INTRODUCTION

Pyrene-labeled lipids have been used extensively to study the molecular dynamics and the structural organization of bilayers and biological membranes. Among these studies are investigations of phospholipid lateral diffusion (Galla and Hartmann, 1980; Jones and Lentz, 1986; Eisinger et al., 1986), spontaneous interbilayer lipid transfer (Roseman and Thompson, 1980; Pownall et al., 1982; Massey et al., 1982, 1984; Frank et at., 1983), protein mediated interbilayer lipid transfer (Wong et al., 1984), transbilayer diffusion (Homan and Pownall, 1985), and the lateral organization of phospholipids in the absence (Somerharju et al., 1985; Hresko et al., 1986) and in the presence of proteins (Weiner et al., 1985; Jones and Lentz, 1986).

The pyrene fluorescence spectrum consists of two components: a violet emission band with vibrational structure characteristic of excited monomers and, at longer wavelengths, a broad structureless emission band characteristic of excited state dimers called excimers (Förster and Kasper, 1955). Birks et al. (1963) used the following scheme to illustrate the various kinetic processes:

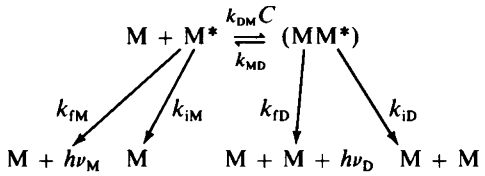

Scheme I

where M* and MM* are excited monomer and excimer molecules, k_{fM} and k_{fD} are the monomer and excimer fluorescence decay parameters, k_{iM} and k_{iD} are the monomer and excimer nonradiative decay parameters, $k_{DM}C$ is the rate constant for excimer formation, k_{DM} is the second order rate constant for excimer formation, C is the probe concentration, and k_{MD} is the rate constant for the regeneration of excited monomer from the dissociation of excimer. The ratio of the excimer-to-monomer fluorescence intensities, E/M, the parameter most frequently measured in pyrene studies, is directly proportional to the collisional

frequency of pyrene molecules and therefore is dependent on the local pyrene concentration. In organic solvents (Birks et al., 1963) and single phase lipid systems (Galla and Sackmann, 1974),

$$E/M = (k_{fD}/k_{fM})k_{DM}C(k_{fD} + k_{iD} + k_{MD})^{-1}. \quad (1)$$

Since pyrene-labeled lipids are widely used in lipid and membrane research, it is important to know how well pyrene-lipid derivatives mimic the physical properties of unlabeled lipid components of the membrane bilayer. A measure of the degree of mimicry is the deviation from ideal mixing of the pyrene-labeled lipid with an unlabeled lipid of interest. We examined one aspect of this question in a recent publication describing studies of the lateral distribution of a pyrene-labeled phosphatidylcholine (PyrPC) in phosphatidylcholine bilayers (Hresko et al., 1986). In this study, E/M measurements were made as a function of temperature in vesicles in which the matrix lipid was dipalmitoyl-, dimyristoyl-, or 1-palmitoyl-2-oleoyl-phosphatidylcholine (DPPC, DMPC, and POPC, respectively). To draw conclusions about the lateral distribution of the probe from the shape of an E/M vs. temperature curve, it was necessary first to simulate E/M vs. temperature curves for systems of known lateral distribution and then compare the simulated curves with the experimentally derived curves. The simulations were carried out using pyrene fluorescence rate parameters determined from phase and modulation data and using local pyrene-lipid concentrations taken from hypothetical phase diagrams. The results indicated that the pyrene-labeled phosphatidylcholine is randomly distributed in pure gel and liquid crystalline phosphatidylcholine bilayers, but in the phase transition region, the probe molecules mix less ideally in DPPC than in DMPC. There is, however, no gel phase immiscibility in these systems.

To investigate further the degree to which pyrene-labeled lipids mimic the physical properties of naturally occurring lipids, we synthesized a pyrene-labeled sphingomyelin (PyrSPM) and a pyrene-labeled glucosylceramide (PyrGlcCer) and studied their distribution in POPC, DPPC, and DMPC by determining E/M as a function of temperature. PyrSPM and PyrGlcCer were chosen because independent evidence suggests that sphingomyelin and glucosylceramide are organized in POPC, DPPC, and DMPC in a more complex manner than is PyrPC. However, the E/M vs. temperature curves for PyrSPM and PyrGlcCer in the three phosphatidylcholine matrices are qualitatively similar to the curves reported for PyrPC in the three matrix phospholipids (Hresko et al., 1986). In an effort to examine further the relationship between the lateral distribution of the probe and the shape of an E/M vs. temperature curve, additional E/M vs. temperature simulations were carried out together with an analysis of Eq. 2 (given below), which relates E/M to the system parameters. The results indicate that E/M vs. temperature curves provide information pertaining to lateral distribution of the labeled lipid only for those systems in which the gel to liquid crystalline phase transition temperature of the matrix lipid is higher than that of the pyrene-labeled probe. However, very little can be known about the system from an E/M vs. temperature curve if the matrix lipid has the lower phase transition temperature. Other independent techniques are necessary under these conditions to characterize the system.

MATERIALS AND METHODS

Materials

Dimyristoyl-, dipalmitoyl-, and 1-palmitoyl-2-oleoyl-phosphatidylcholine were purchased from Avanti Polar Lipids, Inc. (Birmingham, AL). All lipids were checked for purity by thin layer chromatography (TLC) and then stored at −20°C under nitrogen. 10-(1-Pyrenyl)decanoic acid was purchased from Molecular Probes, Inc. (Eugene, OR).

Synthesis of Lipids

1-Palmitoyl-2-[10-(1-pyrenyl)decanoyl]phosphatidylcholine (PyrPC) was synthesized from monoacylphosphatidylcholine and pyrene decanoic acid by the method of Mason et al. (1981). *N*-[10-(1-pyrenyl)decanoyl]sphingomyelin (PyrSPM) was prepared by the procedure of Cohen et al. (1984). *N*-[10(1-pyrenyl)decanoyl]glucocerebroside (PyrGlcCer) was synthesized by the method described by Correa-Freire et al. (1982).

Preparation of Liposomes

Lipids were combined and mixed thoroughly in spectral grade chloroform. The organic solvent was removed and the lipid mixture dried *in vacuo* overnight. Multilamellar vesicles (MLV) were prepared for fluorescence studies in a 10 mM PIPES, 1 mM EDTA, 0.02% NaN_3, pH 7.4 buffer by the method of Bangham et al. (1967). MLV prepared for calorimetric studies were in 50 mM KCl, pH 7.4. Small unilamellar vesicles (SUV) were prepared by cosonicating multilamellar dispersions under nitrogen using the procedure of Barenholz et al. (1977). Large liposomes were separated from SUV by differential ultracentrifugation. SUV were stored overnight under nitrogen above the matrix lipid phase transition temperature (T_m).

Scanning Calorimetry

Calorimetric studies were carried out using a high sensitivity scanning calorimeter of the heat conduction type. The detailed design and operation have been described elsewhere (Suurkuusk et al., 1976). The lipid concentration and sample volume were 15 mM and 0.7 ml, respectively. Samples were incubated overnight in the calorimeter at the desired initial temperature to insure both thermal and system equilibrium. All experiments were in the heating mode at a scanning rate of 10°C/h. Calculations were performed on a CDC Cyber 172 computer.

E/M vs. Temperature Scans

All measurements were carried out on a spectrofluorimeter (model 4800; SLM-Aminco, Urbana, IL). The polarizers were removed to improve signal intensity. The sample cuvette was stirred continuously and temperature was regulated to within ±0.1°C. Sample solutions were flushed with nitrogen for 1 h in gas-tight cuvettes to prevent complications resulting from oxygen guenching. Samples were than incubated at the initial temperature for at least 20 min before measurement. E/M vs. temperature scans were made in the following manner. The sample was excited at 346 nm (2 nm slitwidth) and the emission was monitored at 378 and 470 nm (2 nm slitwidth) using two monochrometers. The ratio of the intensities at 470 nm/378 nm (E/M ratio) and the sample temperature were interfaced directly to a desktop computer (model 9825A; Hewlett-

Packard Co., Palo Alto, CA). The temperature was scanned in the heating mode at a rate of 0.5°C/min using a temperature programmer (model ETP-3; Neslab Instruments, Inc., Portsmouth, NH). A datum point and the temperature were recorded every 25 s. Each datum point was actually an average of 100 E/M values. The pyrene-labeled and the total lipid concentrations were 1.1×10^{-5} and 1.1×10^{-4} M, respectively. Light scattering was negligible at this low lipid concentration. The E/M ratio was also uncorrected for wavelength-dependent changes of the lamp and photomultiplier tubes. Since only relative differences between different probe/lipid mixtures were of interest, corrections were unnecessary.

E/M vs. Temperature Simulations

E/M vs. temperature simulations were carried out using the following equation (Hresko et al., 1986):

$$E/M = \frac{\left[(\sigma_M)\frac{k^I_{DM}C_I k^I_{fD}}{\lambda^I_1\lambda^I_2 k_{fM}} + (1-\sigma_M)\frac{k^{II}_{DM}C_{II}k^{II}_{fD}}{\lambda^{II}_1\lambda^{II}_2 k_{fM}}\right]}{[g_1/\lambda^{II}_1 + g_2/\lambda^{II}_2 + \delta_1/\lambda^I_1 + \delta_2/\lambda^I_2]} \quad (2)$$

where I and II denote the two phases;

$$\sigma_M = C_I\left(\frac{C_T - C_{II}}{C_I - C_{II}}\right)\frac{1}{C_T};\ C_T = \text{total probe/lipid ratio};$$

$$X = k_M + k_{DM}C;\ Y = k_D + k_{MD};$$

$$k_M = k_{fM} + k_{iM};\ k_D = k_{fD} + k_{iD};$$

$$\lambda_{1,2} = (1/2)\{X + Y \mp [(Y-X)^2 = 4k_{DM}k_{MD}C]^{1/2}\};$$

$$g_1 = (1-\sigma_M)\left(\frac{\lambda^{II}_2 - X^{II}}{\lambda^{II}_2 - \lambda^{II}_1}\right);\ \delta_1 = \sigma_M\left(\frac{\lambda^I_2 - X^I}{\lambda^I_2 - \lambda^I_1}\right);$$

$$g_2 = (1-\sigma_M)\left(\frac{X^{II} - \lambda^{II}_1}{\lambda^{II}_2 - \lambda^{II}_1}\right);\ \delta_2 = \sigma_M\left(\frac{X^I - \lambda^I_1}{\lambda^I_2 - \lambda^I_1}\right).$$

It is apparent from Eq. 2 that in a two-component system where two phases coexist, E/M is a function of the following parameters: (*a*) the set of pyrene fluorescence rate parameters corresponding to each phase, k^I_{DM}, k^I_{MD}, k^I_D, k^I_M, $(k_{fD}/k_{fM})^I$, and k^{II}_{DM}, k^{II}_{MD}, k^{II}_D, k^{II}_M, $(k_{fD}/k_{fM})^{II}$; (*b*) the concentration of the probe in the two phases, C_I and C_{II}; and (*c*) the fraction of the probe in the two phases (σ_M) and ($1 - \sigma_M$). Therefore, in the phase transition region where fluid and gel phases coexist, I represents the fluid phase (f) and II represents the gel phase (g). Similarly, in an immiscible gel phase system, I and II denote the two gel phases, which are in equilibrium. Under conditions in which only one phase exists, Eq. 2 simplifies to Eq. 1

RESULTS AND DISCUSSION

Calorimetric Studies on Pyrene-labeled Lipids

Calorimetric measurements were carried out on the neat pyrene-labeled lipids to determine whether the melting properties of lipid analogues mimic those of natural lipid components (data not shown). PyrSPM has a T_m at 43°C and the heat capacity curve has a large width at half maximum (10°C). The phase transition temperature for PyrGlcCer is 55°C and the width of the heat capacity function at half maximum is 5°C. PyrPC has a T_m at ~15°C and a width at half maximum between 2°–2.5°C, which is in agreement with the results of Somerharju et al. (1985). It is apparent that the pyrene moiety lowers the phase transition temperature of the phosphatidylcholine and glucosylceramide but not of the sphingomyelin derivatives. Since pyrene decanoic acid and palmitic acid are approximately equivalent in overall length, PyrPC is structurally similar to DPPC. However, the value of T_m for PyrPC is substantially lower than T_m for DPPC (41°C). This difference reflects the strong dependence of T_m on the acyl moieties seen in phosphatidylcholines (Silvius, 1982). By constrast, the T_m of PyrSPM lies within the range of 35°–45°C found for most sphingomyelins (Cohen et al., 1984; Barenholz et al., 1976). The T_m of PyrGlcCer is 55°C, which is significantly lower than the higher temperature transition (80°C) of natural glucosylceramide (Freire et al., 1980; Barenholz et al., 1983; Maggio et al., 1985) but is close to the temperature of the metastable gel phase to liquid crystalline phase transition of natural glucosylceramide (Freire et al., 1980). It is quite possible that the bulky pyrene moiety prevents PyrGlcCer from undergoing the transformation from the metastable gel phase to the more highly ordered gel conformation.

E/M vs. Temperature Scans

POPC Matrix. At temperatures above the POPC phase transition temperature (−5°C; Silvius, 1982), E/M increases smoothly with increasing temperature for PyrPC/POPC (Fig. 1 *A*), PyrSPM/POPC (Fig. 1 *B*), and PyrGlcCer/POPC (Fig. 1 *C*) multilamellar liposomes. The E/M vs. temperature curves described above are heating scans. The cooling scan for PyrSPM in

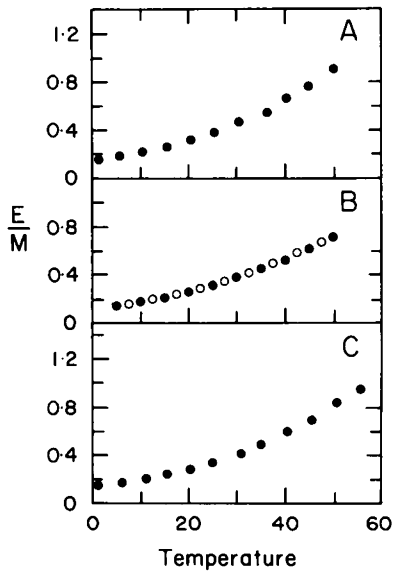

FIGURE 1 E/M vs. temperature curves obtained in the heating mode for (*A*) PyrPC/POPC MLV (●); (*B*) PyrSPM/POPC MLV (●); (*C*) PyrGlcCer/POPC MLV (●). A cooling scan for PyrSPM/POPC MLV (○) is also presented in *B*. All experiments were carried out at 10 mol% pyrene lipid.

POPC is nearly identical to the heating scan (Fig. 1 *B*). This indicates that the system is close to or at equilibrium.

DPPC Matrix. The E/M vs. temperature plots for PyrPC/DPPC (Fig. 2 *A*), PyrSPM/DPPC (Fig. 2 *B*), and PyrGlcCer/DPPC (Fig. 2 *C*) MLV are all N-shaped with a minimum at the DPPC phase transition temperature (41°C; Silvius, 1982) and a maximum between 35° and 38°C. The heating and cooling scans for PyrSPM in DPPC (Fig. 2 *B*) are nearly identical indicating that the sample is essentially at equilibrium during the measurements.

DMPC Matrix. E/M vs. temperature plots for PyrPC/DMPC (Fig. 2 *D*), PyrSPM/DMPC (Fig. 2 *E*), and PyrGlcCer/DMPC (Fig. 2 *F*) MLV are not N-shaped but show a small break several degrees below the DMPC T_m. Also shown in Fig. 2 *D* is an E/M vs. temperature plot for PyrPC/DMPC SUV. The break is more apparent in MLV than in SUV systems. This is probably due to packing differences between the two types of vesicles.

In liquid crystalline matrices, it can be seen in Figs. 1 and 2 that E/M increases smoothly with temperature for all systems. That no dramatic changes in slope near the phase transition of the probe are observed suggests that excimer formation is diffusion-controlled and the probe is randomly dispersed in the bilayer above the matrix lipid T_m. For certain systems this conclusion is supported by independent evidence. Oxygen-quenching experiments on PyrPC in POPC (Chong and Thompson, 1985) and spontaneous lipid transfer studies on PyrPC in DMPC, PyrSPM in DPPC, PyrSPM in DMPC (Roseman and Thompson, 1980; Frank et al., 1983), and PyrGlcCer in POPC (M. Wong; unpublished results) indicate the probe is randomly distributed in a fluid phospholipid matrix.

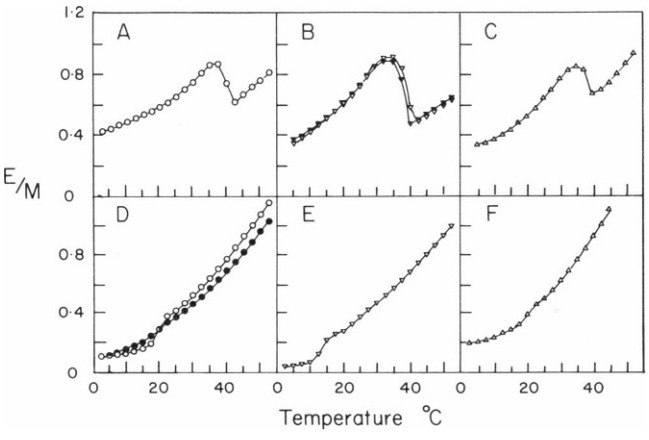

FIGURE 2 E/M vs. temperature curves obtained in the heating mode for (*A*) PyrPC/DPPC MLV (○); (*B*) PyrSPM/DPPC MLV (▽); (*C*) PyrGlcCer/DPPC MLV (△); (*D*) PyrPC/DMPC MLV (○) and SUV (●); (*E*) PyrSPM/DMPC MLV (▽); (*F*) PyrGlcCer/DMPC MLV (△). A cooling scan for PyrSPM/DPPC MLV (▼) is also presented in *B*. All experiments were carried out at 10 mol% pyrene lipid.

However, for several systems this conclusion is at odds with other information. Spontaneous lipid transfer studies on PyrSPM in POPC, PyrGlcCer in DMPC, tritiated glucocerebroside in DMPC, and tritiated glucocerebroside in DPPC (Frank et al., 1983; Correa-Freire et al., 1982), and oxygen-quenching experiments on PyrSPM in POPC (Chong and Thompson, 1985) all suggest that a gel phase rich in the probe coexists with a liquid crystalline phase rich in the matrix phospholipid below the phase transition temperature of the probe.

In a DPPC matrix, the E/M vs. temperature curves for PyrPC in DPPC, PyrSPM in DPPC, and PyrGlcCer in DPPC are all N-shaped. It has been shown (Hresko et al., 1986) using E/M vs. temperature simulations that an N-shaped curve indicates that the mixing of the probe in the phase transition region is nonideal, which means the probe preferentially distributes in fluid domains rather than in gel domains. Simulations also indicate that if E/M increases with decreasing temperature in the gel state, the system is immiscible in the gel state. It is assumed that if E/M decreases with decreasing temperature in the gel state, the system is miscible. Based on this information, the E/M vs. temperature data indicate that PyrPC, PyrSPM, and PyrGlcCer mix nonideally in DPPC in the phase transition region, but they are randomly distributed in DPPC in the gel state. The conclusion about PyrGlcCer in DPPC, however, is not in agreement with calorimetric experiments carried out on glucosylceramide–DPPC mixtures (Correa-Freire et al., 1979; Barenholz et al., 1983), which suggest that at low concentrations of glucosylceramide (<50 mol%) these two components are immiscible in the gel state.

In a DMPC matrix, the E/M vs. temperature curves for PyrPC in DMPC, PyrSPM in DMPC, and PyrGlcCer in DMPC are not N-shaped but have a small break several degrees below the DMPC T_m. It has been shown by E/M vs. temperature simulations (Hresko et al., 1986) that a break in an E/M vs. temperature curve indicates that the pyrene-labeled lipid does not distribute preferentially in either fluid or gel domains in the phase transition region. Spontaneous lipid transfer experiments on PyrGlcCer in DMPC (Correa-Freire et al., 1982), however, suggest that a gel phase enriched in PyrGlcCer exists in fluid bilayers of DMPC below the PyrGlcCer T_M. This is contrary to the interpretation of the E/M vs. temperature function.

A comparison of the phase transition temperatures of the pyrene-labeled lipid and the matrix lipid in each of the nine systems described above is shown in Table I. This information may be helpful in the following discussion.

Interrelations between E/M vs. Temperature Curves and Phase Diagrams. The discrepancies cited above between the interpretations of E/M vs. temperature curves and the interpretations based on other independent techniques can be resolved by an analysis of Eq. 2. This equation gives $E/M(T)$ in terms of the concentrations of

TABLE I
COMPARISON OF THE PHASE TRANSITION TEMPERATURES OF THE PYRENE-LABELED LIPID AND THE MATRIX LIPID IN THE NINE EXPERIMENTAL SYSTEMS.

Pyrene-labeled lipid ($T_p^{\ddagger}$ in °C)	Matrix lipid (T_m^* in °C)		
	POPC(−5)	DMPC(23)	DPPC(41)
PyrPC (15)	$T_m < T_p$	$T_m > T_p$	$T_m > T_p$
PyrSPM (43)	$T_m < T_p$	$T_m < T_p$	$T_m \leq T_p$
PyrGlcCer (55)	$T_m < T_p$	$T_m < T_p$	$T_m < T_p$

*T_m, gel to liquid crystalline phase transition temperature of the matrix lipid.

‡T_p, gel to liquid crystalline phase transition temperature of the pyrene-labeled lipid.

the pyrene-labeled lipids and the fractions of this lipid in the two coexisting phases. In this section, we perform this analysis and examine the predictions derived from it by means of E/M vs. temperature simulations based on Eq. 2.

It is clear from the experimental data that E/M is a smoothly increasing function of increasing temperature both in homogeneous gel and in liquid crystalline phases. In the mixed phase regime, however, E/M can either be a smoothly increasing function of the temperature (Fig. 1, *B* and *C*) or can show a marked discontinuity (Fig. 2, *A* and *C*). The physical basis for this behavior of the $E/M(T)$ function in the two phase region emerges from the following analysis.

The temperature derivative of Eq. 2 is

$$\frac{d(E/M)}{dT} = \sum_i \left[\frac{\partial(E/M)}{\partial k_i^{I}} \cdot \frac{dk_i^{I}}{dT} + \frac{\partial(E/M)}{\partial k_i^{II}} \cdot \frac{dk_i^{II}}{dT} \right] + \frac{\partial(E/M)}{\partial C_I} \cdot \frac{dC_I}{dT} + \frac{\partial(E/M)}{\partial C_{II}} \cdot \frac{dC_{II}}{dT}, \quad (3)$$

where the summation goes through the different indices of the rate constants (ff, DM, D, MD, M; $k_{fD}/k_{fM} = k_{ff}$) as defined in Materials and Methods. The numerical analysis of the partial derivatives show that

$$\left.\begin{aligned} \frac{\partial(E/M)}{\partial C_I} \\ \frac{\partial(E/M)}{\partial C_{II}} \end{aligned}\right\} \begin{cases} > 0, & \text{if } C_{II} < C_T \\ < 0, & \text{if } C_{II} > C_T \end{cases} \quad \begin{cases} > 0, & \text{if } C_I < C_T \\ < 0, & \text{if } C_I > C_T. \end{cases} \quad (4)$$

The summation term in Eq. 3 reflects the temperature dependences of the rate constants for each phase and their effect on the E/M function. As described above, both in homogeneous gel and liquid crystalline phases ($|dC_{II}/dT|$ and $|dC_I/dT| = 0$), E/M increases smoothly with increasing temperature. The second and third terms indicate the degree of mixing of the two components in the system. These two terms at the solidus and liquidus lines of a phase diagram have either a large negative or positive value if the solidus or liquidus lines are close to horizontal ($|dC_{II}/dT|$ or $|dC_I/dT| \leq \infty$). This causes an abrupt decrease or increase, respectively, in the E/M function. However, if the liquidus and solidus lines are close to vertical ($|dC_{II}/dT|$ or $|dC_I/dT| \approx 0$), then the summation term is dominant.

Let us now examine in detail the relationship between the $E/M(T)$ function and the phase diagram for several systems, first in the gel–liquid crystalline mixed phase region and then in the gel–gel mixed phase region. In each case, the predictions of the analysis are tested by constructing simulated E/M vs. temperature curves based on suitable hypothetical phase diagrams and Eq. 2. All simulations are carried out at 10 mol% pyrene lipid with the gel and liquid crystalline rate parameters for PyrPC in DPPC as reported by Hresko et al. (1986).

Gel–Liquid Crystalline Mixed Phase Region: Matrix T_m > Probe T_m. In this two phase region where fluid and gel phases coexist, I represents the fluid phase (f) and II represents the gel phase (g). If the mixture is nonideal (see Fig. 3 *A;* the total system concentration, C_T, is denoted by the vertical line [*b*] at the right), the large negative values of $(dC_f/dT)_{T_f}$ at the liquidus lines cause an abrupt change in E/M at $T <$ matrix T_m. T_f is the temperature of the liquidus curve at $C = C_T$. It is clear from an examination of the simulated $E/M(T)$ curves shown in Fig. 3 *B*, which are based on the phase diagrams depicted in Fig. 3 *A*, that the closer the liquidus curve is to

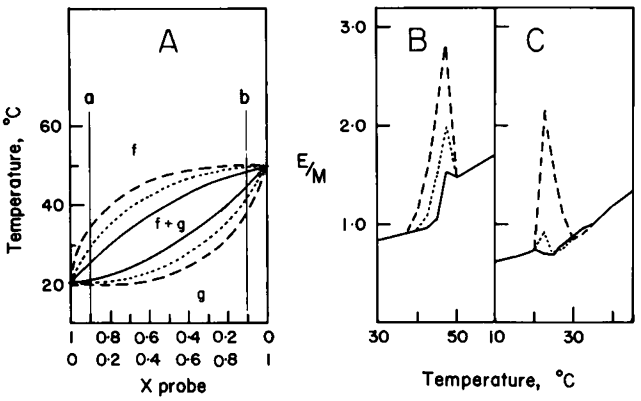

FIGURE 3 (*A*) Three hypothetical phase diagrams for two component miscible systems that differ in their ideality of mixing in the phase transition region: (——) nearly ideal, (----) less ideal, and (— —) least ideal. f is the fluid phase, g is the gel phase, and f + g is the mixed phase. Line *a* represents the pyrene lipid composition (10 mol%) at which the E/M vs. temperature simulations were carried out for systems in which the pyrene lipid T_m is higher than the matrix lipid T_m. Line *b* represents the pyrene lipid composition (10 mol%) at which the E/M vs. temperature simulations were carried out for systems in which the matrix lipid T_m is higher than the pyrene lipid T_m. (*B* and *C*) Simulated E/M vs. temperature curves based on the three phase diagrams shown in *A*. (*B*) Simulated $E/M(T)$ curves for systems in which the matrix lipid T_m is higher than the pyrene lipid T_m. (*C*) Simulated $E/M(T)$ curve for systems in which the pyrene lipid T_m is higher than the matrix lipid T_m. The method used to simulate the $E/M(T)$ curves is described in Results and Discussion.

being horizontal, the sharper the change in E/M. Usually, the less ideal the mixture is, the closer the liquidus curve is to horizontal. The physical basis for the abrupt changes in $E/M(T)$ at the liquidus line can be understood in the following terms. Since the systems are completely miscible, above the phase transition region C_f is equal to the total system concentration ($C_T = 0.1$), while C_g is equal to C_T below the phase transition region. As the temperature is lowered below the liquidus line, C_f increases sharply as a fraction of the matrix phospholipid undergoes a fluid–gel transition, while the majority of the probe remains in the fluid phase. This large increase in C_f coupled with the fact that the majority of the probe is in the fluid phase overcomes the temperature dependence of the pyrene rate parameters and therefore E/M increases as the temperature is lowered below the liquidus line. This is the case for 10 mol% PyrPC in DPPC (Fig. 2 *A*) where E/M increases abruptly as the temperature is lowered below the liquidus line (41°C). It can be seen in Fig. 3 *B* that the less ideal the system is, the greater the increase in C_f and the larger the percentage of probe remaining in the fluid phase. This results in a larger increase in the E/M ratio. It has been shown previously (Hresko et al., 1986) that PyrPC in DMPC is closer to ideality than PyrPC in DPPC and therefore the change in E/M at the respective matrix lipid T_m is much smaller in the case of PyrPC in DMPC (Fig. 2 *D*).

However, as the temperature is lowered below the solidus line, no abrupt change in the E/M ratio is observed. In contrast to $(dC_f/dT)_{T_f}$ at the liquidus curve, which is very large, $(dC_g/dT)_{T_g}$ at the solidus line is much smaller. T_g is the temperature of the solidus curve at $C = C_T$. As the temperature is lowered in the mixed phase region, C_f becomes very large, but the fraction of probe in the fluid phase (σ_M) decreases to zero near the solidus line. Since the decrease of σ_M is not abrupt with decreasing temperature, it therefore does not have a significant effect on the $E/M(T)$ curve. This can be seen by examination of the temperature derivative of the fraction of the system that is liquid crystalline:

$$\left(\frac{d\sigma_M}{dT}\right)_{T_g} = \left(\frac{\partial\sigma_M}{\partial C_f}\right)_{\substack{C_g=C_T\\C_f=C_f(T_g)}} \cdot \left(\frac{dC_f}{dT}\right)_{T_g} + \left(\frac{\partial\sigma_M}{\partial C_g}\right)_{\substack{C_g=C_T\\C_f=C_f(T_g)}} \cdot \left(\frac{dC_g}{dT}\right)_{T_g}$$

$$= -\frac{C_f}{C_T(C_f - C_T)} \cdot \left(\frac{dC_g}{dT}\right)_{T_g} \approx -\frac{1}{C_T} \cdot \left(\frac{dC_g}{dT}\right)_{T_g}. \quad (5)$$

However, $|(dC_g/dT)_{T_g}|$ is not very large as is shown in Fig. 3 *A*. Therefore, the contribution of liquid crystalline domains to the E/M function near the solidus line is negligible. At the same time as the temperature is lowered in the mixed phase region, the fraction of probe in the gel phase increases and C_g approaches C_T. However, as the temperature is lowered below the solidus line, the change in C_g is small and therfore the E/M function is dominated by the temperature dependence of the rate constants.

Gel–Liquid Crystalline Mixed Phase Region: Probe T_m > Matrix T_m. If the probe T_m is higher than the matrix T_m and the mixture is nonideal but miscible, the solidus curve is close to horizontal at C_T and thus $(dC_g/dT)_{T_g} \lesssim \infty$. This condition is shown in Fig. 3 *A* with C_T denoted by the vertical line (*a*) on the left. The large positive value of $(dC_g/dT)_{T_g}$ causes an abrupt increase in E/M at the solidus line. Note that $\partial(E/M)/\partial C_g > 0$, too (see Eq. 4). In general, the closer the solidus curve is to horizontal at C_T, the sharper the increase in E/M. Physically, close to the solidus curve where gel domains dominate over the amount of liquid crystalline domains, the small probe concentration in the gel phase increases from C_T to a much higher value within a very small temperature interval, resulting in the sudden increase of E/M.

In contrast to the situation at the solidus curve, close to the liquidus curve there is no abrupt change in $E/M(T)$. This is the case because on crossing the liquidus curve at (C_T, T_f) gel domains that have a much higher probe concentration than C_T disappear. But since the amount of these domains does not decrease strongly at $T < T_f$, only a slow change in E/M results. The temperature derivative of the amount of gel domains is

$$\left[\frac{d(1-\sigma_M)}{dT}\right]_{T_f} = \left[\frac{\partial(1-\sigma_M)}{\partial C_g}\right]_{\substack{C_g=C_g(T_f)\\C_f=C_T}} \cdot \left(\frac{dC_g}{dT}\right)_{T_f} + \left[\frac{\partial(1-\sigma_M)}{\partial C_f}\right]_{\substack{C_g=C_g(T_f)\\C_f=C_T}} \cdot \left(\frac{dC_f}{dT}\right)_{T_f}$$

$$= \frac{C_g}{C_T(C_T - C_g)}\left(\frac{dC_f}{dT}\right)_{T_f} \approx -\frac{1}{C_T}\left(\frac{dC_f}{dT}\right)_{T_f}, \quad (6)$$

where $(dC_f/dT)_{T_f}$ is not a significantly large value (see Fig. 3 *A*; C_T at the left side of the figure).

This interpretation of the $E/M(T)$ function is in accord with the assymmetry of the simulated and measured E/M peaks shown in Figs 3, *B* and *C* and 2, *A*, *B*, and *C*, respectively. The peaks are always sharper on the side of the matrix T_m. According to the analysis, the sharp change of E/M is expected to be close to T_{matrix}.

A strongly nonideal phase diagram does not always give rise to an abrupt change in $E/M(T)$ for a system in which the probe T_m > matrix T_m. This is shown by the phase diagram in Fig. 4 *A*, which was chosen because it probably resembles the shape of the phase diagram for PyrSPM in POPC. Spontaneous lipid-transfer and oxygen-quenching studies carried out at a relatively low concentration of probe suggest that a gel phase rich in PyrSPM exists below the PyrSPM T_m (Frank et al., 1983; Chong and Thompson, 1985). Therefore, the phase transition region must be very broad, lying between roughly 45°C and −5°C. The simulated E/M vs. temperature curve is shown in Fig. 4 *B*. E/M decreases almost linearly with decreasing temperature beginning at temperatures that are above the liquidus line to temperatures near the solidus line. There is a slight increase in E/M as the temperature is lowered below the

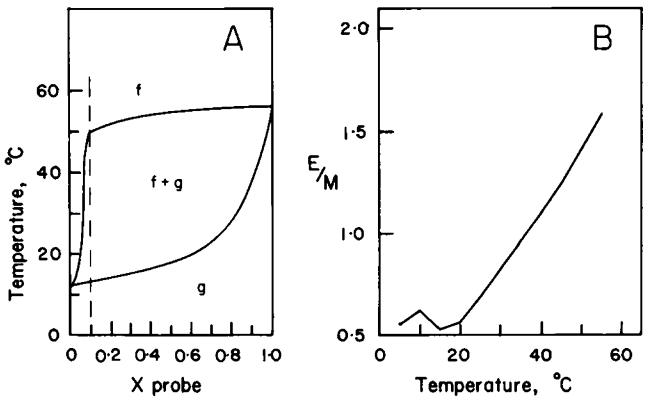

FIGURE 4 (*A*) Phase diagram for a hypothetical two component miscible system in which the T_m of the pyrene lipid is higher than the T_m of the matrix lipid. The mixed phase region is very broad and nonideal in this case. f is the fluid phase, g is the gel phase, and f + g is the mixed phase. *Dashed line*, the pyrene lipid composition (10 mol%) at which the $E/M(T)$ simulation shown in *B* was carried out. The method used to simulate the curve is described in Results and Discussion.

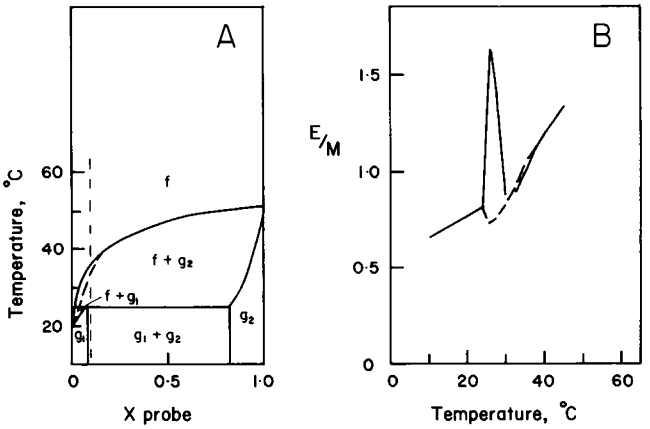

FIGURE 5 (*A*) Phase diagrams for two hypothetical two component peritectic systems in which the T_m of the pyrene lipid is higher than the matrix lipid T_m. The two phase diagrams are identical except that the liquidus line of one phase diagram (— —) is shifted slightly to the right relative to the other diagram (——). f is the fluid phase, g is the gel phase. f + g_1 and f + g_2 are mixed gel–liquid crystalline phases. g_1 is a homogeneous gel phase, g_2 is the second homogeneous gel phase, and g_1 + g_2 is a mixed gel phase. *Vertical dashed line*, the pyrene lipid composition (10 mol%) at which the E/M vs. temperature simulations shown in *B* were carried out. The method used to simulate the $E/M(T)$ curves is described in Results and Discussion.

solidus line, but then E/M continues to decrease with decreasing temperature. In the preceding discussion, it was shown that E/M does not increase as the temperature is lowered across the liquidus line because the number of probe molecules undergoing a fluid-to-gel transition is too small to be observed in the E/M ratio. Assuming that the phase diagram used in this simulation resembles that of PyrSPM in POPC, the E/M vs. temperature curve for PyrSPM in POPC would be expected to simply increase with increasing temperature from 1°C to 50°C. E/M should only increase with decreasing temperature near the solidus line, but since the solidus line is near the POPC T_m (−5°C) and, therefore, outside the temperature range examined, E/M is not observed experimentally to increase with decreasing temperature. In fact, the actual E/M vs. temperature curve for 10 mol% PyrSPM in POPC simply increases with increasing temperature. The same result is observed for 10% PyrGlcCer in DPPC (Fig. 2 *C*) and PyrGlcCer in DMPC (Fig. 2 *F*) above the matrix lipid T_m (see Table I for T_m's). Therefore, gel domains cannot be detected in a fluid matrix from the shape of an E/M vs. temperature curve even though they can be detected by spontaneous lipid transfer and oxygen quenching.

Another example that demonstrates that the shape of an $E/M(T)$ curve cannot be simply predicted from phase diagrams if the probe T_m > matrix T_m is shown in Fig. 5 *B*. The curves in Fig. 5 *B* are based on the peritectic phase diagrams in Fig. 5 *A*. The simulations indicate that if the liquidus curve is shifted slightly to the right, the E/M vs. temperature curve changes dramatically from an N-shaped curve to one that is relatively flat in the phase transition region. This is the case because $|dC_g/dT|$ and $|dC_f/dT|$ are relatively small everywhere in the peritectic $T_m < T$ probe T_m temperature interval and therefore it is difficult to predict from the phase diagrams which term in Eq. 3 will be the leading one. Peritectic T_m is the temperature of the horizontal line in the peritectic diagram.

Gel-Gel Mixed Phase Region. The phase lines of the mixed gel phase are marked by $C_{g1}(T)$ and $C_{g2}(T)$, where $C_{g1} > C_{g2}$ (see Fig. 6 *A*).

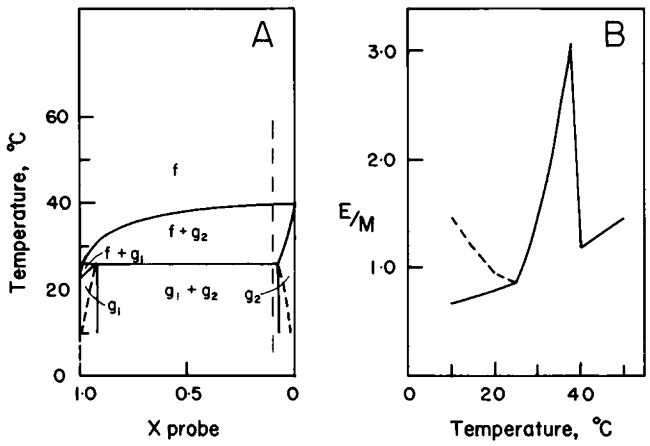

FIGURE 6 (*A*) Phase diagrams for two hypothetical two component peritectic systems in which the T_m of the matrix lipid is higher than the T_m of the pyrene lipid. The two phase diagrams are identical except in the mixed gel phase region. The gel phase boundary lines are vertical (——) in one case but show a mirror symmetry in the other case (— —). f is the fluid phase. g is the gel phase, f + g_1 and f + g_2 are mixed gel–liquid crystalline phases. g_1 is a homogeneous gel phase, g_2 is another homogeneous gel phase, and g_1 + g_2 is a mixed gel phase. *Vertical dashed line*, the pyrene lipid composition (10 mol%) at which the E/M vs. temperature simulations shown in *B* were carried out. The method used to simulate the $E/M(T)$ curves is described in Results and Discussion.

To analyze the temperature dependence of E/M, we make the following substitution in Eq. 3:

$$C_{\mathrm{I}} = C_{\mathrm{g1}} \text{ and } C_{\mathrm{II}} = C_{\mathrm{g2}}$$

Obviously, if the phase lines are close to vertical, i.e., $dC_{g1}/dT \approx dC_{g2}/dT \approx 0$, the second and the third terms in Eq. 3 are negligible and the temperature dependences of the rate constants k_i determine the value of E/M. Therefore, E/M increases with increasing temperature. This will usually be the case with peritectic and eutectic systems.

If the phase lines are not vertical but show mirror symmetry, that is $C_{g1} = 1 - C_{g2}$, the form of Eq. 3 will be simpler:

$$\frac{d(E/M)}{dT} = 2\sum_i \left[\frac{\partial(E/M)}{\partial k_i^{\mathrm{I}}} \cdot \frac{dk_i^{\mathrm{I}}}{dT}\right] + \left[\frac{\partial(E/M)}{\partial C_{g2}} - \frac{\partial(E/M)}{\partial C_{g1}}\right] \cdot \frac{dC_{g2}}{dT}. \quad (7)$$

Here we take into consideration that $k_i^{\mathrm{I}} = k_i^{\mathrm{II}}$ for all rate constants in the gel–gel mixed phase region and because of the symmetry of the phase lines:

$$\frac{dC_{g1}}{dT} = -\frac{dC_{g2}}{dT}.$$

Since $dC_{g2}/dT > 0$ and according to Eq. 4 $\partial(E/M)/\partial C_{g2} < 0$, $\partial(E/M)/\partial C_{g1} > 0$, the second term in Eq. 7 always reduces the slope of the E/M curve in the gel–gel mixed phase region. Depending on the value of the first (positive) and second (negative) terms, the slope of the E/M curve can be positive or negative in the gel–gel mixed phase region (see Fig. 6, *A* and *B*). Therefore, our original assumption stated in the Results is incorrect, that is, if E/M decreases with decreasing temperature in the gel state, the system is miscible. This explains why the $E/M(T)$ curve for 10% PyrGlcCer in DPPC (Fig. 2 *C*) increases with increasing temperature in the gel state even though the calorimetric studies indicate that low concentrations of glucosylceramide in DPPC are immiscible in the gel phase.

CONCLUSIONS

The preceding analysis of the relationships between the $E/M(T)$ functions and the corresponding phase diagrams of two component systems leads to the following general conclusions.

(*a*) Gel phase immiscibility can be detected from the shape of an E/M vs. temperature curve only if E/M increases with decreasing temperature in the gel state. However, if E/M decreases with decreasing temperature in the gel state, the system may either be miscible or immiscible in the gel phase. An independent technique must then be used to determine the lateral distribution of the probe in the gel state.

(*b*) The relationship between the shape of an E/M vs. temperature curve and the lateral distribution of the probe in the phase transition region is dependent upon which component has a higher phase transition temperature, the matrix lipid or the probe. The simpler case occurs when the matrix lipid T_m is higher than the T_m of the probe. The simulations show that a break in an $E/M(T)$ curve indicates that the probe can mix almost ideally between the fluid and gel domains in the phase transition region. An N-shaped E/M vs. temperature curve, however, indicates the mixing is nonideal, which means the probe preferentially distributes in fluid domains. The less ideal the mixing is, the larger the increase in E/M as the temperature is lowered below the liquidus line.

(*c*) A more complex situation occurs when the T_m of the probe is higher than that of the matrix lipid. The E/M vs. temperature curve for a nonideal system may have either a break or an N-shape. There are no simple rules regarding the lateral distribution of the probe and the shape of the E/M vs. temperature curve if the probe T_m is higher than the matrix lipid T_m. Other techniques such as spontaneous lipid transfer and oxygen quenching, which are more sensitive, must be used to draw conclusions about the lateral distribution of the probe under these conditions.

Since E/M vs. temperature curves can be used to determine the lateral distribution of the pyrene-labeled probe in a bilayer unambiguously for only those systems in which the matrix lipid T_m is higher than the probe T_m, it is therefore necessary to know the phase transition temperature of the probe. The T_m of probe can be determined calorimetrically or from an E/M vs. temperature curve of the neat material (Somerharju et al., 1985). It is important to note, however, that we have not examined using simulations those systems in which the matrix lipid and the probe have similar phase transition temperatures such as PyrSPM in DPPC. Since PyrSPM has a very broad phase transition that extends over temperatures both above and below the DPPC T_m, it is difficult to predict whether information about the lateral distribution can be obtained from the shape of an $E/M(T)$ curve.

We wish to thank Dr. Martin Wong for his assistance with the calorimetric measurements and Dr. Frances A. Stephenson for drawing the graphics.

The work was supported by National Institutes of Health grants GM-14628 and HL-17576. R. C. Hresko was supported by National Institutes of Health training grant GM-07294.

Received for publication 22 August 1986 and in final form 8 January 1987.

REFERENCES

Bangham, A. D., J. de Gier, and G. D. Greville. 1967. Osmotic properties and water permeability of phospholipid liquid crystals. *Chem. Phys. Lipids.* 1:225–246.

Barenholz, Y., J. Suurkuusk, D. Mountcastle, T. E. Thompson, and R. L. Biltonen. 1976. A calorimetric study of the thermotropic behavior of

aqueous dispersions of natural and synthetic sphingomyelins. *Biochemistry*. 15:2441–2447.

Barenholz, Y., D. Gibbes, B. J. Litman, J. Goll, and T. E. Thompson. 1977. A simple method for the preparation of homogeneous phospholipid vesicles. *Biochemistry*. 16:2806–2810.

Barenholz, Y., E. Freire, T. E. Thompson, M. C. Correa-Freire, D. Bach, and I. R. Miller. 1983. Thermotropic behavior of aqueous dispersions of glucosylceramide-dipalmitoyl-phosphatidylcholine mixtures. *Biochemistry*. 22:3497–3501.

Birks, J. B., D. J. Dyson, and I. H. Munro. 1963. 'Excimer' fluorescence II. Lifetime studies of pyrene solutions. *Proc. R. Soc. Lond. A. Math. Phys. Sci.* 275:575–588.

Chong, P. L.-G., and T. E. Thompson. 1985. Oxygen quenching of pyrene-lipid fluorescence in phosphatidylcholine vesicles. A probe for membrane organization. *Biophys. J.* 47:613–621.

Cohen, R., Y. Barenholz, S. Gatt, and A. Dagan. 1984. Preparation and characterization of well defined D-erythrosphingomyelins. *Chem. Phys. Lipids*. 35:371–384.

Correa-Freire, M. C., E. Freire, Y. Barenholz, R. L. Biltonen, and T. E. Thompson. 1979. Thermotropic behavior of monoglucocerebroside-dipalmitoylphosphatidylcholine multilamellar liposomes. *Biochemistry*. 18:442–445.

Correa-Freire, M. C., Y. Barenholz, and T. E. Thompson, 1982. Glucocerebroside transfer between phosphatidylcholine bilayers. *Biochemistry*. 21:1244–1248.

Eisinger, J., J. Flores, and W. P. Petersen. 1986. A milling crowd model for local and long-range obstructed lateral diffusion. Mobility of excimeric probes in the membrane of intact erythrocytes. *Biophys. J.* 49:987–1001.

Förster, Th., and K. Kasper. 1955. Ein Konzentrationsumschlag der Fluoreszenz des Pyrens. *Z. Elektrochem.* 59:976–980.

Frank, A., Y. Barenholz, D. Lichtenberg, and T. E. Thompson. 1983. Spontaneous transfer of sphingomyelin between phospholipid bilayers. *Biochemistry*. 22:5647–5651.

Freire, E., D. Bach, M. C. Correa-Freire, I. Miller, and Y. Barenholz. 1980. Calorimetric investigation of the complex phase behavior of glucocerebroside dispersions. *Biochemistry*. 19:3662–3665.

Galla, H.-J., and E. Sackmann. 1974. Lateral diffusion in the hydrophobic region of membranes: use of pyrene excimers as optical probes. *Biochim. Biophys. Acta*. 339:103–115.

Galla, H.-J., and W. Hartmann. 1980. Excimer-forming lipids in membrane research. *Chem. Phys. Lipids*. 27:199–219.

Homan, R., and H. J. Pownall. 1986. Dependence of transbilayer diffusion of pyrene labeled phospholipids on head group composition. *Biophys. J.* 49(2, Pt.2):517a. (Abstr.)

Hresko, R. C., I. P. Sugár, Y. Barenholz, and T. E. Thompson. 1986. Lateral distribution of a pyrene-labeled phosphatidylcholine in phosphatidylcholine bilayers: fluorescence phase and modulation study. *Biochemistry*. 25:3813–3823.

Jones, M. E., and B. R. Lentz. 1986. Phospholipid lateral organization in synthetic membranes as monitored by pyrene-labeled phospholipids: effects of temperature and prothrombin fragment 1 binding. *Biochemistry*. 25:567–574.

Maggio, B., T. Ariga, J. M. Sturtevant, and R. K. Yu. 1985. Thermotropic behavior of glycosphingolipids in aqueous dispersions. *Biochemistry*. 24:1084–1092.

Mason, J. T., A. V. Broccoli, and C. Huang. 1981. A method for the synthesis of isomerically pure saturated mixed-chain phosphatidylcholines. *Anal. Biochem.* 113:96–101.

Massey, J. B., A. M. Gotto, and H. J. Pownall. 1982. Kinetics and mechanism of the spontaneous transfer of fluorescent phosphatidylcholines between apolipoprotein-phospholipid recombinants. *Biochemistry*. 21:3630–3636.

Massey, J. B., D. Hickson, H. S. She, J. T. Sparrow, D. P. Via, A. M. Gotto, and H. J. Pownall, 1984. Measurement and prediction of the rates of spontaneous transfer of phospholipids between plasma lipoproteins. *Biochim. Biophys. Acta*. 794:274–280.

Pownall, H. J., D. Hickson, A. M. Gotto, and J. B. Massey. 1982. Kinetics of spontaneous and plasma-stimulated sphingomyelin transfer. *Biochim. Biophys. Acta*. 712:169–176.

Roseman, M. A., and T. E. Thompson. 1980. Mechanism of the spontaneous transfer of phospholipids between bilayers. *Biochemistry*. 19:439–444.

Silvius, J. R. 1982. Thermotropic phase transitions of pure lipids in model membranes and their modification by membrane proteins. *In* Lipid-Protein Interactions. Vol. 2. P. Jost and D. M. Griffith, editors. John Wiley & Sons, Inc., New York. 239–281.

Somerharju, P. J., J. A. Virtanen, K. K. Eklund, P. Vainio, and P. K. J. Kinnunen. 1985. 1-palmitoyl-2-pyrenedecanoyl glycerophospholipids as membrane probes: evidence for regular distribution in liquid-crystalline phosphatidylcholine vesicles. *Biochemistry*. 24:2773–2781.

Suurkuusk, J., B. R. Lentz, Y. Barenholz, R. L. Biltonen, and T. E. Thompson. 1976. A calorimetric and fluorescent probe study of the gel-liquid crystalline phase transition in small, single-lamellar dipalmitoylphosphatidylcholine vesicles. *Biochemistry*. 15:1393–1401.

Wiener, J. R., R. Pal, Y. Barenholz, and R. R. Wagner. 1985. Effect of the vesicular stomatitis virus matrix protein on the lateral organization of lipid bilayers containing phosphatidylglycerol: use of fluorescent phospholipid analogues. *Biochemistry*. 24:7651–7658.

Wong, M., R. E. Brown, Y. Barenholz, and T. E. Thompson. 1984. Glycolipid transfer protein from bovine brain. *Biochemistry*. 23:6498–6505.